Inorganic Chemistry

Article

pubs.acs.org/IC

Crowning of Coinage Metal Pyrazolates: Double-Decker Homo- and Heteronuclear Complexes with Synergic Emissive Properties

Mattia Veronelli, Nicole Kindermann, Sebastian Dechert, Steffen Meyer, and Franc Meyer*

Institut für Anorganische Chemie, Georg-August-Universität Göttingen, Tammannstrasse 4, D-37077 Göttingen, Germany

Supporting Information

ABSTRACT: A new pyrazole ligand with flexible thioether chelate arms was synthesized and was used to obtain an unprecedented class of hexanuclear coinage metal complexes of general formula $[MM'L]_3Y_3$ (M, M′ = Cu, Ag, Au; Y = OTf, BF_4). Three of them were characterized by X-ray crystallography, namely, homometallic $[Ag_2L]_3(OTf)_3$ and $[Ag_2L]_3(BF_4)_3$ as well as heterometallic $[CuAgL]_3(OTf)_3$, revealing that the classical $[M(\mu\text{-pz})]_3$ core is crowned by a second deck of S-bound M′ ions. Depending on the solvent, these oligonuclear systems undergo rapid dynamics and show cation−anion aggregation in solution, which has been investigated by DOSY and temperature dependent NMR spectroscopy. Preliminary luminescence data for selected hexametallic $[MM'L]_3Y_3$ complexes show that the combination of ligand-directed intramolecular and supramolecular d^{10} metal ion interactions in the solid state gives rise to synergic emissive properties that allow for a selective addressing of different emission wavelengths.

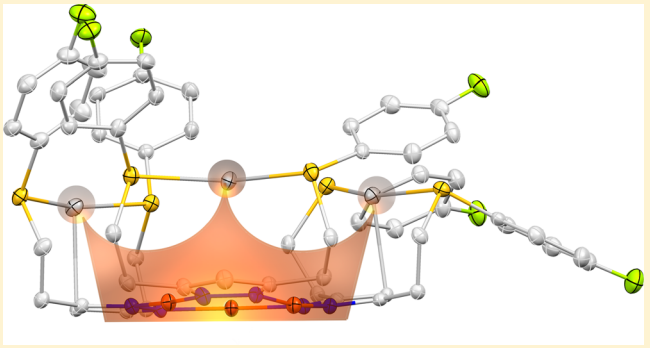

INTRODUCTION

Pyrazoles are popular ligands in coordination chemistry,[1,2] and their complexes with monovalent coinage metal ions have attracted widespread interest as supramolecular synthons[3] because of, *inter alia*, their propensity to form π-acid/π-base stacks,[4] their attractive luminescence properties,[5] and their potential catalytic applications.[6,7] Depending on the metal ion used and the substituents at the pyrazole heterocycle, coinage metal pyrazolates adopt different oligo- and polynuclear structures with the trimeric ring $[M(\mu\text{-pz})]_3$ (pz = pyrazolate) being the most prominent motif.[8] Stacking of those metallamacrocycles as shown in **I** (Figure 1) is commonly observed in the solid state, and intermolecular contacts between the closed-shell d^{10} metal ions as well as intramolecular interactions are known to govern the photophysical characteristics of this class of compounds.[5,9−11]

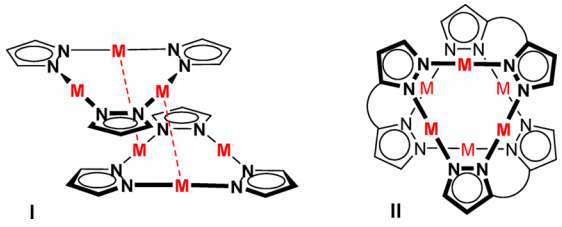

Figure 1. Stacking of pyrazolate coinage metal trimers often observed in the solid state (**I**) and hexametallic double-decker complexes based on linked bis(pyrazolato) ligands (**II**).

With the goal of maximizing and directing the intermetallic interactions, or for building nanocages that can encapsulate guest molecules, recent studies have targeted the synthesis of pairs of $[M(\mu\text{-pz})]_3$ trimers using linked bis(pyrazolato) ligands as clips (e.g., **II**).[12] We communicated the use of ligands with chelating arms in positions 3 and 5 of the pyrazole,[13] in particular some pyrazole/thioether hybrid ligands HL′ (Figure 2),[14] for synthesizing octanuclear heterometallic complexes **III**

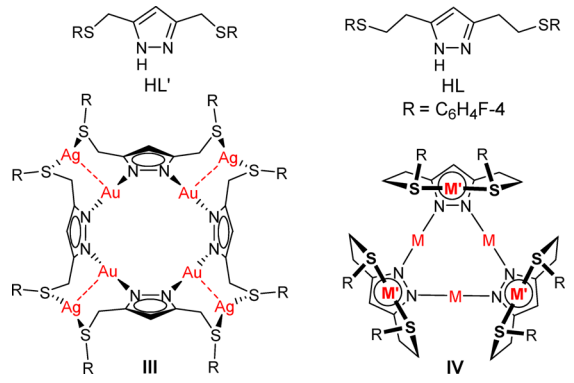

Figure 2. Left: pyrazolate/thioether ligands HL′ and recently reported octanuclear Au_4Ag_4 complexes **III**.[15] Right: new pyrazolate/thioether ligand HL and hexanuclear double-decker complexes **IV** described in this work.

Received: January 23, 2014
Published: February 6, 2014

   dx.doi.org/10.1021/ic5001792 | *Inorg. Chem.* 2014, 53, 2333−2341

in which the inner $[Au(\mu\text{-pz})]_4$ ring is framed by a peripheral ring of Ag^+ ions.[15] Because of the short length of the thioether side arms, the outer Ag^+ ions in **III** are constrained to lie within the plane of the central golden square, supported by in-plane inter-ring metallophilic interactions. While this added a new turn to coinage metal pyrazolate chemistry,[15] we reasoned that longer and more flexible chelate arms might allow for the (usually preferred) arrangement of additional metal ions above or below the $[M(\mu\text{-pz})]_x$ metallocycles. Following this concept we introduce here a new pyrazole/thioether ligand HL (Figure 2) that features elongated side arms, and we show that this ligand leads to a novel series of hexanuclear homo- and heterometallic complexes **IV** in which the $[M(\mu\text{-pz})]_3$ core is crowned by a second set of metal ions, giving rise to promising synergic emissive properties.

RESULTS AND DISCUSSION

The synthesis of the new proligand HL is sketched in Scheme 1. It is based on the recently reported 3-step synthesis of 3,5-

Scheme 1. Synthesis of the New Proligand HL

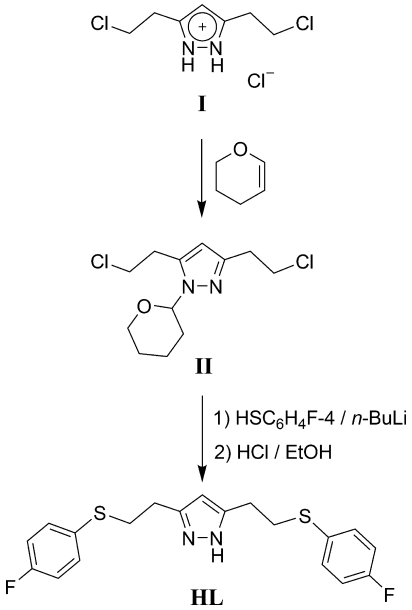

di(chloroethyl)pyrazole hydrochloride (**I**) from dimethyl dioxopimelate,[16] which has been adapted with minor modifications (see the Supporting Information for details). Now the pyrazole-NH of **I** is first protected by introducing a tetrahydropyranyl (thp) group[17] to give **II**, and subsequent nucleophilic substitution using lithiated 4-fluorothiophenol followed by deprotection yields the new pyrazole/thioether hybrid ligand HL. The particular 4-fluorophenyl substituent on the thioether chelate arms was chosen to make use of ^{19}F NMR spectroscopy as an analytical probe for studying the resulting complexes in solution.

Treatment of HL with an excess of Ag_2O in CH_2Cl_2 leads to the formation of the trimeric silver(I) complex $[AgL]_3$; subsequent transmetalation with $AuCl(SMe_2)$ gives the corresponding gold complex $[AuL]_3$. Direct reaction of HL with $[Cu(CH_3CN)_4](BF_4)$ in the presence of triethylamine leads instead to a mixture of two species identified by field-desorption mass spectrometry (FD-MS) to be $[CuL]_3$ and $[CuL]_4$ (Figures S16 and S17 in the Supporting Information). Coinage metal pyrazolates $[M(\mu\text{-pz})]_x$ are known to exist, in certain cases, as mixtures of oligomers in solution, the preferred ring size depending on the steric demand of the substituents and other factors.[8] ^1H diffusion-ordered spectroscopy (DOSY) NMR of the mixture $[CuL]_x$ in $CDCl_3$ is consistent with this interpretation (Figure 3 and Figure S1 in the Supporting Information), and ^1H NMR at variable temperatures shows that the two complexes are in equilibrium (with thermodynamic parameters $\Delta H = -46.6$ kJ·mol^{-1} and $\Delta S = -178.6$ J·mol^{-1}·K^{-1} for $4[CuL]_3 \leftrightarrow 3[CuL]_4$; see Figure 3 for the van't Hoff plot, Figure S2 in the Supporting Information, and the Supporting Information for details). Isolation of a single species $[CuL]_x$ was so far unsuccessful.

No significant changes of the ^1H NMR chemical shifts for the thioether substituents of HL were observed upon complex formation for any of the present complexes $[ML]_x$ (M = Cu, Ag, Au). This is evidence that in all these homometallic complexes the thioether substituents are dangling and are not involved in metal coordination, but are potentially available for binding additional coinage metal ions.

Treatment of complexes $[ML]_x$ with stochiometric amounts (x equiv) of AgOTf or CuOTf·$^1/_2C_6H_6$ in CH_2Cl_2 yielded hexanuclear complexes of general formula $[MM'L]_3(OTf)_3$ (where M is coordinated to the pyrazolate-N and M′ to the thioether-S) for a total of four different metal ion combinations (M = Cu, M′ = Cu, Ag; M = M′ = Ag; M = Au, M′ = Ag). Their formation was first indicated by FD mass spectra, since the base peak in the FD-MS spectra is represented either by the

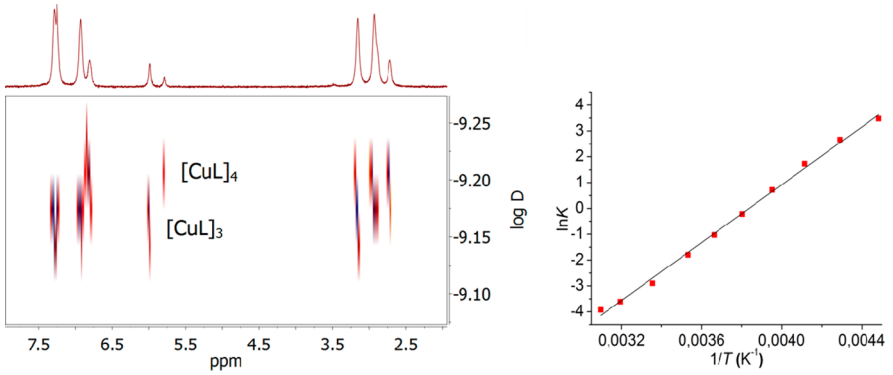

Figure 3. ^1H DOSY spectrum of the mixture $[CuL]_3/[CuL]_4$ in $CDCl_3$ (left) and plot of ln K vs $1/T$ ($K = [CuL]_4^3/[CuL]_3^4$, right). See Supporting Information for further details.

dx.doi.org/10.1021/ic5001792 | Inorg. Chem. 2014, 53, 2333−2341

species $[M_3M'_2L_3(OTf)]^+$ and/or by the species $[M_3M'_3L_3(OTf)_2]^+$ (see Figures S18−S25 in the Supporting Information). The Cu-only system again is an exception, since FD mass spectra suggested the presence of two species $[Cu_2L]_3(OTf)_3$ and $[Cu_2L]_4(OTf)_4$, which likely are in equilibrium similar to the findings for the precursor complexes $[CuL]_x$ (for FD-MS spectra and enlargement of the most characteristic peaks see Figures S23−S25 in the Supporting Information).

Single crystals suitable for X-ray diffraction could be obtained for two complexes, namely, heterometallic $[CuAgL]_3(OTf)_3$ and homometallic $[Ag_2L]_3(OTf)_3$. Their molecular structures are very similar, and the structure of the cation $\{[CuAgL]_3\}^{3+}$ is shown in Figure 4 as an example (see Figure S39 in the Supporting Information for the molecular structure of $\{[Ag_2L]_3\}^{3+}$). As anticipated, the nearly planar trimeric core of the precursor complexes with bridging pyrazolates and two-coordinate metal ions, $[M(\mu\text{-pz})]_3$, is fully conserved in the hexametallic species. Intratrimer distances are found in the typical range 3.10−3.25 Å between the Cu ions in $[CuAgL]_3(OTf)_3$ and 3.39−3.43 Å between the Ag ions in $[Ag_2L]_3(OTf)_3$. It is important to note, however, that $[CuAgL]_3(OTf)_3$ was obtained from the reaction of trimeric $[AgL]_3$ with $CuOTf\cdot{}^1/_2C_6H_6$, though surprisingly an inner $[Cu(\mu\text{-pz})]_3$ core is found in the product. Reshuffling of the metal ions has obviously occurred, and in the heterometallic hexanuclear complexes the different metal ions finally arrange according to the Pearson principle with Ag^+ favoring the softer thioether-S donors and Cu^+ ending up N-coordinated in the $[Cu(\mu\text{-pz})]_3$ ring. The required lability of the pyrazolate-based $[ML]_3$ entities is well established[18] and is evidenced for the present system by the equilibrium between $[ML]_3$ and $[ML]_4$ in case of M = Cu, as discussed above.

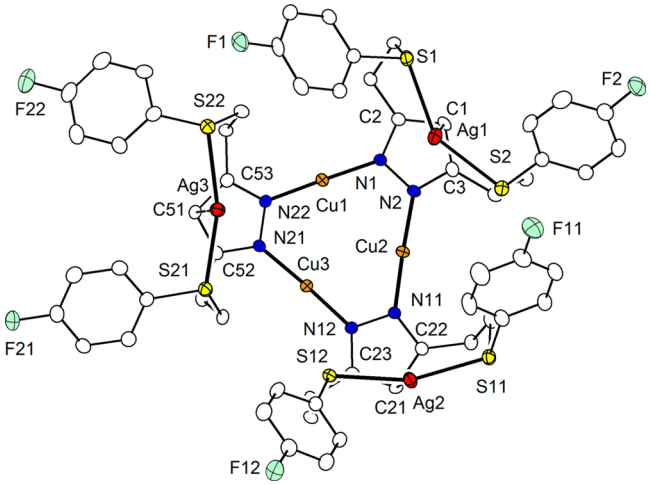

Figure 4. ORTEP plot (30% probability thermal ellipsoids) of the molecular structure of the cation of $[CuAgL]_3(OTf)_3$. For clarity all hydrogen atoms and triflates are omitted. For atom distances and bond angles, see the Supporting Information.

The three additional M′ ions, i.e., Ag^+ in both $\{[CuAgL]_3\}^{3+}$ and $\{[Ag_2L]_3\}^{3+}$, are all found on one side of the $[M(\mu\text{-pz})]_3$ core and are each coordinated by thioether-S of the two chelate arms attached to one $[L]^-$ ligand. They are located directly above the pyrazolate ring of that ligand with rather short Ag−C contacts, though offset from the normal to the center of the ring. In most cases the shortest distance is found between the Ag^+ and the pyrazolate-C^4 atom (2.60−2.73 Å and 2.52−3.07 Å, respectively, for $\{[CuAgL]_3\}^{3+}$ and $\{[Ag_2L]_3\}^{3+}$), followed by $C^{3/5}$, while all Ag···N^{pz} contacts are >3 Å. The Ag^+-pyrazolate binding motif thus is best described as η^1 or η^3. A similar binding situation has been previously described for pyrazolate-based silver complexes containing platinum or palladium.[19−21] However, displacement of the Ag^+ above the pyrazolate ring seems to be facile: in $[Ag_2L]_3(OTf)_3$, Ag6 is located almost above the center of the ring with a relatively short Ag···centroid distance which is close to a η^5 coordination, though all individual contacts are >3 Å. The η^1 or η^3 bonding interaction found for most of the outer Ag^+ ions is likely responsible for a bending of the S−Ag−S angles, since those Ag^+ ions with short Ag−C distances show smaller S−Ag−S angles. Accordingly the angle S21−Ag6−S22 in $[Ag_2L]_3(OTf)_3$ (η^5 coordination of Ag6) is closer to linearity than all other S−Ag−S angles (Figure 4, Figure S39 in the Supporting Information).

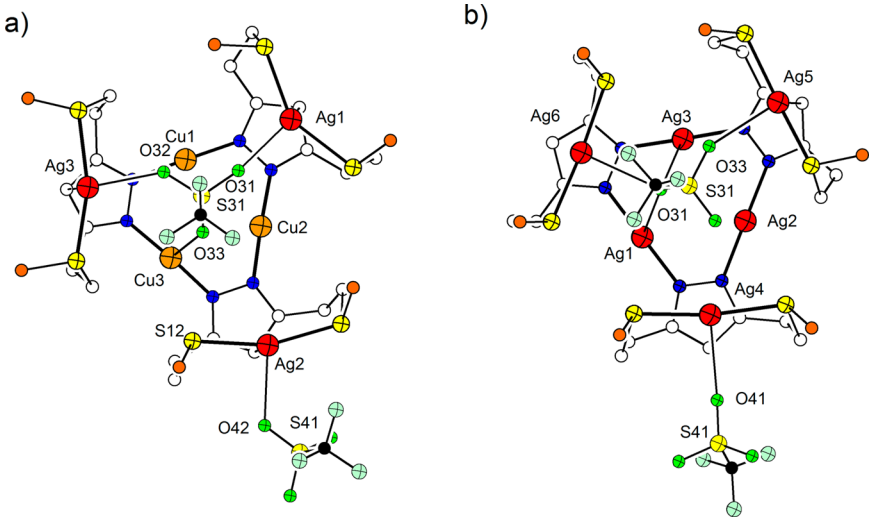

Figure 5. Top views onto the central hexametallic cores of $[CuAgL]_3(OTf)_3$ (a) and $[Ag_2L]_3(OTf)_3$ (b) emphasizing metal···triflate contacts <3 Å; all 4-fluorophenyl substituents are omitted for clarity.

dx.doi.org/10.1021/ic5001792 | Inorg. Chem. 2014, 53, 2333−2341

In both $[MAgL]_3(OTf)_3$ (M = Cu, Ag) the triflates do not merely serve as counteranions, but one triflate is sitting above the $[M(\mu\text{-pz})]_3$ metallacycle on the same side as the S-bound Ag^+. It interacts, via the triflate-O, with several M and M′ metal ions (shortest Ag−O distances of 2.65 Å in $[Ag_2L]_3(OTf)_3$ and 2.50 Å in $[CuAgL]_3(OTf)_3$, shortest Cu−O distance 2.74 Å in the latter). The disposition of this triflate is similar in the two complexes, but not identical. This indicates that the triflates may readily reorient above the $[M(\mu\text{-pz})]_3$ metallacycle, and it suggests a fluxional behavior in solution (see below for NMR studies). In $[CuAgL]_3(OTf)_3$, two Ag−O distances are remarkably shorter than the third one (2.50 Å vs 4.21 Å) and the three contacts between triflate-O and the inner Cu are in the range 2.74−3.51 Å (Figures 5a and S43 in the Supporting Information). For $[Ag_2L]_3(OTf)_3$ the metal−O distances are more uniform: for the S-coordinated Ag they lie in the range 2.65−3.04 Å, while for the pyrazolate-bound Ag they are in the narrow range 2.91−3.16 Å (Figures 5b and S44 in the Supporting Information).

Interestingly, in the crystals both $[MAgL]_3(OTf)_3$ (M = Cu, Ag) show a centrosymmetric "face to face" arrangement of two hexametallic $\{[MAgL]_3\}^{3+}$ entities, with two intermolecular M···M contacts typical for d^{10} coinage metal pyrazolates (compare **I**, Figure 1). The distance between the $[M(\mu\text{-pz})]_3$ planes is 2.89 Å in $[CuAgL]_3(OTf)_3$ (Figure 6) and 2.96 Å in

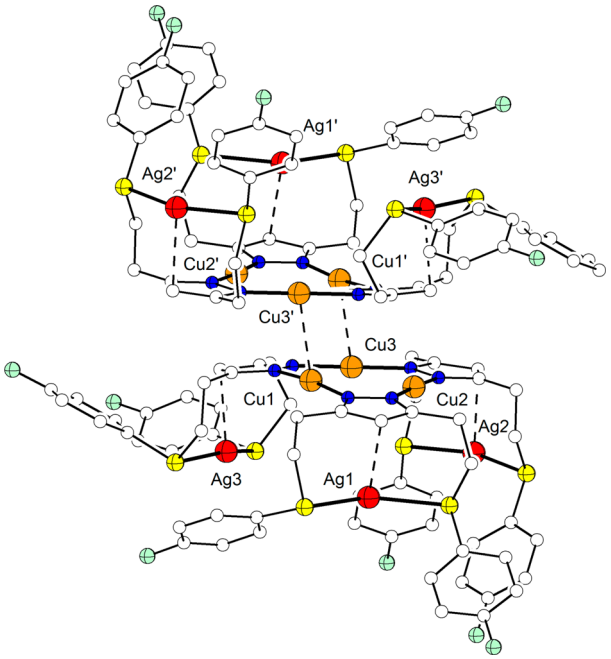

Figure 6. Part of the solid state structure of $[CuAgL]_3(OTf)_3$ emphasizing the dimerization of two hexanuclear $\{[CuAgL]_3\}^{3+}$ entities via short Cu1···Cu3′ contact (2.891(1) Å). Symmetry operations used to generate equivalent atoms: (′) $1-x, 1-y, 1-z$.

$[Ag_2L]_3(OTf)_3$ (Figure S42 in the Supporting Information), which is close to or even shorter than the sum of van der Waals radii (2.80 Å for Cu and 3.44 Å for Ag).[22] These unsupported metallophilic M···M contacts are among the shortest so far reported for coinage metal pyrazolates.[23,24]

In order to investigate whether the aggregates of hexametallic $\{[MAgL]_3\}^{3+}$ entities are also present in solution, and whether the triflates remain associated with the complexes, extensive NMR spectroscopic studies were performed using crystalline material of $[MAgL]_3(OTf)_3$ (M = Cu, Ag). In all cases, ^1H NMR spectra of $CDCl_3$ solutions showed only broad peaks, suggesting fast dynamic equilibria that are difficult to rationalize. As an example, the results for $[Ag_2L]_3(OTf)_3$ will be briefly described here (Figures S3−S7 in the Supporting Information). Its ^1H NMR spectrum recorded at room temperature revealed only a single set of broad signals, reflecting the absence of diastereotopic CH_2 protons that would be expected if chelate arms of the ligands were arranged as found in the solid state. At lower temperatures additional broad peaks appear in the aliphatic region. However, the number of signals at −50 °C is higher than expected for a structure with the three M′ metal ions on the same side of the $[Ag(\mu\text{-pz})]_3$ core and with 3-fold symmetry (which should give rise to four doublets of doublets of doublets for the CH_2 protons). A more complicated scenario in solution was thus assumed, likely with additional isomers present in which only two of the M′ ions are located on one side of the $[Ag(\mu\text{-pz})]_3$ plane while the third M′ is on the other side. Fast dynamic equilibria at room temperature then lead to a time-averaged apparent planar structure on the NMR time scale. Also the ^{19}F NMR spectra show a splitting of the signals for the C_6H_4F-4 substituents at low temperatures (Figure S4 in the Supporting Information). To further elucidate the role of the anions, ^{19}F DOSY was performed. For complexes $[MM'L]_3(OTf)_3$ in $CDCl_3$, this technique gave the same diffusion coefficients for the triflates and the ligands (with values between 5.0×10^{-10} and 4.0×10^{-10} $m^2\ s^{-1}$; see Figure 7 and Figures S8 and S10 in the Supporting Information) clearly showing that the triflates remain tightly associated with the complex in solution.[25] However, this supramolecular association is highly solvent dependent: for both $[CuAgL]_3(OTf)_3$ and $[Ag_2L]_3(OTf)_3$, ^1H and ^{19}F NMR spectra recorded in acetone-d_6 show a single set of relatively sharp peaks at room temperature, with partially resolved J couplings (Figure S5 in the Supporting Information). Furthermore, in the case of acetone solutions ^{19}F DOSY revealed a significantly larger diffusion coefficient for the triflates than for the ligands (2.0×10^{-9} $m^2\ s^{-1}$ versus 1.1×10^{-9} $m^2\ s^{-1}$ for $[CuAgL]_3(OTf)_3$; 1.2×10^{-9} $m^2\ s^{-1}$ versus 7.1×10^{-10} $m^2\ s^{-1}$ for $[Ag_2L]_3(OTf)_3$; Figure 7 and Figures S8−S11 in the Supporting Information). This reflects that dissociation of the triflates occurs in more polar and potentially coordinating solvents, likely giving solvent separated ion pairs. However, at lower temperatures the ^1H and ^{19}F NMR resonances again split into a number of signals, which indicates that $[Ag_2L]_3(OTf)_3$ undergoes dynamic processes even in acetone-d_6 solution (Figures S6 and S7 in the Supporting Information).

In order to corroborate the above interpretation of the variable temperature NMR (VT-NMR) results, we synthesized the hexanuclear complexes $[MAgL]_3(BF_4)_3$ (M = Ag, Au) from $[ML]_3$ and $AgBF_4$, anticipating that the BF_4^- anion might interact less with the metal ions and so would exert less influence on the overall structure. The complex $[Ag_2L]_3(BF_4)_3$ was successfully crystallized and subjected to X-ray diffraction analysis (molecular structure of the cation $\{[Ag_2L]_3\}^{3+}$ shown in Figure 8 and Figure S40 in the Supporting Information).

Many of the structural features are the same for $[Ag_2L]_3(BF_4)_3$ and $[Ag_2L]_3(OTf)_3$: a $[Ag(\mu\text{-pz})]_3$ core consisting of a roughly planar Ag_3N_6 metallacycle (Ag···Ag distances of 3.44−3.46 Å) is crowned by three additional Ag^+ ions bound to two thioether-S, and with short Ag−pyrazolate contacts (d(Ag···C[4]) in the range 2.55−2.69 Å). However, in

dx.doi.org/10.1021/ic5001792 | Inorg. Chem. 2014, 53, 2333−2341

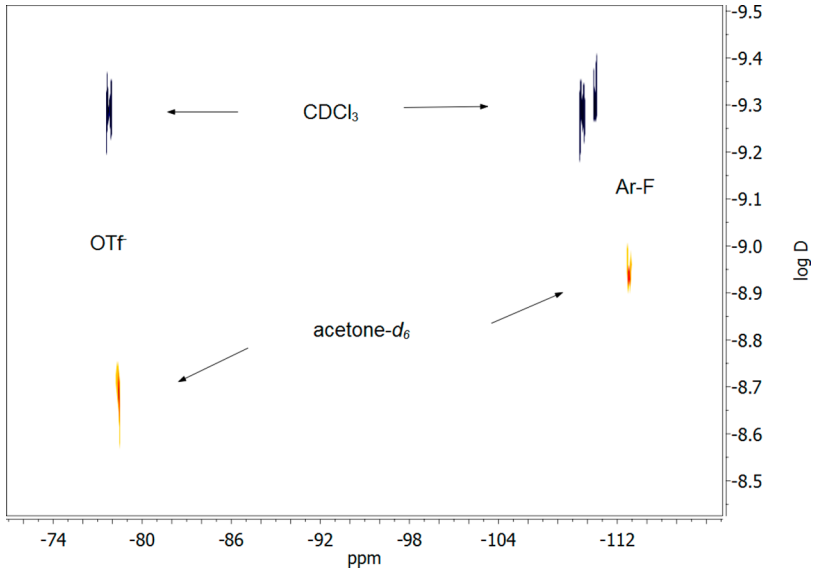

Figure 7. Overlay of ^{19}F DOSY spectra of $[CuAgL]_3(OTf)_3$ recorded in $CDCl_3$ (black) and acetone-d_6 (red), showing the signal for triflate (around −78 ppm) and the 4-fluorophenyl group (around −110/−112 ppm).

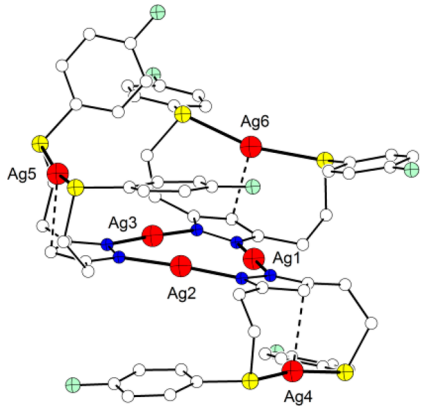

Figure 8. Solid state molecular structure of the cation of $[Ag_2L]_3(BF_4)_3$. For clarity all hydrogen atoms and BF_4^- are omitted. For atom distances and bond angles, see the Supporting Information.

the case of $[Ag_2L]_3(BF_4)_3$ two of the outer S-bound Ag^+ are located above and one is located below the central $[Ag(\mu\text{-pz})]_3$ plane, thus representing the isomer with noncrystallographic C_s symmetry that was proposed on the basis of the NMR experiments. The three BF_4^- are found more distant from the $\{[Ag_2L]_3\}^{3+}$ complex (shortest Ag···F distance 2.81 Å; Figure S45 in the Supporting Information) than the triflates in $[Ag_2L]_3(OTf)_3$, likely reflecting the different strength of the Ag···F and Ag···O interactions. Having the thioether chelate arms and the outer Ag^+ on different sides of the $[Ag(\mu\text{-pz})]_3$ core prevents any aggregation of the hexanuclear units, and consequently intermolecular metal−metal interactions such as the ones seen in Figure 6 are not present.

^{1}H NMR spectra of complexes $[MAgL]_3(BF_4)_3$ (M = Ag, Au) were only recorded in acetone-d_6 because of low solubility in less polar media. A single set of relatively sharp signals with well resolved J couplings was observed at room temperature (Figure S12 in the Supporting Information), in accordance with a time-averaged apparent planar structure on the NMR time scale. ^{19}F DOSY spectra reveal a much larger diffusion coefficient for the BF_4^- anions than for the ligands (1.6×10^{-9} m^2 s^{-1} versus $6.9 \times 10^{-10}/6.1 \times 10^{-10}$ m^2 s^{-1} for M = Ag/Au, respectively), which is in line with solvent separated ion pairs in solution. The more ionic situation for complexes $[MAgL]_3(BF_4)_3$ compared to $[MAgL]_3(OTf)_3$ explains the insolubility of the former in nonpolar solvents such as CH_2Cl_2 and $CHCl_3$. However, even in the case of $[Ag_2L]_3(BF_4)_3$ a

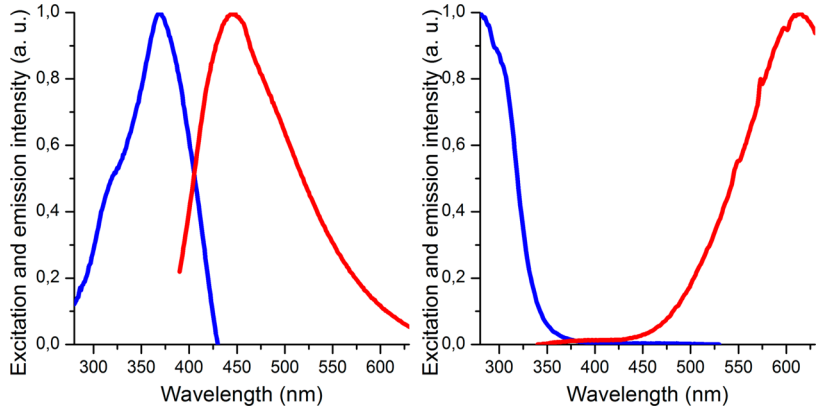

Figure 9. Excitation (blue) and emission (red) spectra of the compounds $[Ag_2L]_3(OTf)_3$ (left) and $[Cu_2L]_3(OTf)_3$ (right) (in solid state).

dx.doi.org/10.1021/ic5001792 | Inorg. Chem. 2014, 53, 2333−2341

dynamic equilibrium of several isomers is obvious from the variable temperature ^{1}H NMR spectra that show splitting into numerous resonances upon cooling (see Figure S13 in the Supporting Information).

Preliminary studies on the luminescence properties were performed for solid (powder) samples of the series of novel crownlike double-decker complexes $[MM'L]_3Y_3$ (Y = OTf, BF_4). Upon exposure to UV radiation all of them show intense emission in the visible region. Though the exact nature of the electronic transitions involved in these processes remains to be investigated, from comparison of the various complexes it is clear that the metal ions play a dominant role. Considering first the homometallic hexanuclear complexes, distinct spectra were obtained for $[Ag_2L]_3(OTf)_3$ and $[Cu_2L]_3(OTf)_3$. The former emits at 445 nm (λ_{ex} 370 nm), the latter at 615 nm (λ_{ex} 320 nm) (Figure 9, Figures S29 and S31 in the Supporting Information). A difference of 35 nm between the emission maxima of hexasilver complexes $[Ag_2L]_3(OTf)_3$ (445 nm) and $[Ag_2L]_3(BF_4)_3$ (410 nm) furthermore shows that the anions and their interaction with the metal ions play a role as well (Figure S30 in the Supporting Information).

Results for the heterometallic complexes $[MM'L]_3Y_3$ suggest hybrid photophysical properties originating from both types of metals ions, i.e., from the $[M(\mu\text{-pz})]_3$ core and the S-bound upper M′ deck. In all cases two peaks are observed in the emission spectra, and their relative intensities are strongly dependent on the excitation wavelength used. The two emission maxima are relatively close for $[AuAgL]_3(OTf)_3$ (λ_{max} at 419 and 441 nm; Figure S33 in the Supporting Information) and $[AuAgL]_3(BF_4)_3$ (λ_{max} at 448 and 505 nm; Figure S34 in the Supporting Information), but appear at significantly different energy for $[CuAgL]_3(OTf)_3$. Upon excitation of $[CuAgL]_3(OTf)_3$ at 320 nm, an emission peak at 620 nm is observed with a small shoulder at around 430 nm. When exciting at longer wavelength, the intensity of the first peak drops while the second rises to become the predominant band at λ_{ex} of 365 nm (Figure 10).[26]

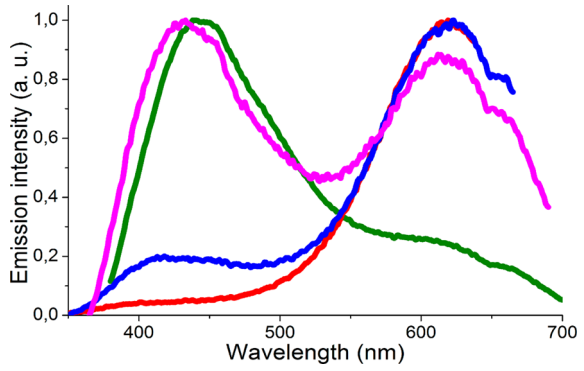

Figure 10. Normalized emission spectra of $[CuAgL]_3(OTf)_3$ at different excitation wavelength: 320 nm (red), 335 nm (blue), 350 nm (magenta), 365 nm (green) (in solid state).

Obviously the presence of two types of metal ions in the heterometallic double-decker complexes $[MM'L]_3Y_3$ allows for addressing different electronic transitions and luminescence signatures. It should be noted that the emission band around 430 nm for $[CuAgL]_3(OTf)_3$ is reminiscent of the band for $[Ag_2L]_3(OTf)_3$ (Figure 9, left), while the band around 620 nm is similar to the emission of $[Cu_2L]_3(OTf)_3$ (Figure 9, right). Variation of the excitation wavelength thus permits selectively choosing an emission in the orange or violet-blue regions for the hybrid material $[CuAgL]_3(OTf)_3$.[27] Our interpretation, *viz.*, that the two emission bands originate from the different types of metals ions (Ag versus Cu) arranged in the two decks of the heterometallic complex, is also supported by photophysical studies of the corresponding homometallic complexes $[Ag_2L]_3(OTf)_3$ and $[Cu_2L]_3(OTf)_3$ at different excitation wavelengths. In both latter cases the scanning of λ_{ex} merely results in a variation of intensity of the corresponding main emission peak, while rising of other significant emission peaks is not observed (Figures S36 and S37 in the Supporting Information), in clear contrast to $[CuAgL]_3(OTf)_3$.

Besides, it is important to note that emissions of the trinuclear starting complexes $[ML]_3$ (M = Ag, Au) are centered in the UV, while the mixture $[CuL]_3/[CuL]_4$ emits with λ_{max} 584 nm (Figures S26−S28 in the Supporting Information). In all cases the addition of the M′ upper deck causes a significant bathochromic shift of the emission, reflecting synergic emissive properties of the hexanuclear compounds.

CONCLUSIONS

In conclusion, the results reported herein represent a significant extension of coinage metal pyrazolate chemistry, demonstrating a new strategy to obtain hybrid luminophores, both homo- and heterometallic, with synergic emissive properties. Attractive characteristics arise from the crowning of the classical $[M(\mu\text{-pz})]_3$ core with a second metal ion deck, directed by proper choice of chelate arms attached to the pyrazole, and thus by the combination of common *supramolecular* (cf. Figure 6) and novel ligand-enforced *intramolecular* (cf. Figure 4) interactions of the d^{10} coinage metal ions. Construction of multinuclear systems by adding further donor sites to the chelate arms is an attractive perspective. This and a detailed analysis of the synergic photophysical properties of the heterometallic $[MM'L]_3Y_3$ complexes are currently pursued in our laboratory.

EXPERIMENTAL SECTION

Methods and Materials. All ligand syntheses were carried out under an anaerobic and anhydrous atmosphere of dry nitrogen by using standard Schlenk techniques. **I** was prepared in close analogy to the reported method (see ref 16 and the Supporting Information). THF was dried over sodium in the presence of benzophenone, and MeOH and CH_2Cl_2 were dried over CaH_2 and distilled prior to use. NMR spectra were recorded on Bruker Avance 300 MHz and Bruker DRX 500 MHz spectrometers. Chemical shifts are reported in ppm relative to residual proton and carbon signal of the solvent ($CDCl_3$, δ_H = 7.26, δ_C = 77.16 ppm; acetone-d_6, δ_H = 2.05, δ_C = 29.84 ppm; D_2O, δ_H = 4.79 ppm; DMSO-d_6, δ_H = 2.50, δ_C = 39.52). EI mass spectra were recorded with a Finnigan MAT 8200. ESI mass spectra were recorded with an Applied Biosystems API 2000 and a BRUKER HCT ultra. FD mass spectra were recorded with a JEOL AccuTOF GCv. Luminescence spectra were recorded using a Horiba-Jobin-Yvon Fluorolog-3 instrument, equipped with an R928 photomultiplier tube from Hamamatsu and a 450 W Xe lamp as an excitation source. Elemental analyses were performed by the analytical laboratory of the Institute of Inorganic Chemistry at Georg-August-University using an Elementar Vario EL III instrument. Details of the X-ray crystallographic structure determinations can be found in the Supporting Information. CCDC 965215, 965216, and 965216 contain the supplementary crystallographic data for this paper. These data can be obtained free of charge from The Cambridge Crystallographic Data Centre via http://www.ccdc.cam.ac.uk/data_request/cif.

3,5-Bis(chloroethyl)-1-(tetrahydropyran-2-yl)-1*H*-pyrazole (II). 3,5-Bis(chloroethyl)pyrazole hydrochloride **I**[16] (1.05 g, 4.57 mmol) was suspended in CH_2Cl_2 (30 mL). Under stirring 3,4-

dx.doi.org/10.1021/ic5001792 | *Inorg. Chem.* 2014, 53, 2333−2341

dihydro-2*H*-pyran (1.5 mL, 5.5 mmol) was added dropwise. The resulting solution was left at room temperature for 24 h and was subsequently hydrolyzed with Na_2CO_3 (5 g) in water (100 mL). The aqueous layer was extracted with CH_2Cl_2 (2 × 30 mL). The organic phases were collected, dried over $MgSO_4$ and concentrated in vacuo. The resulting oil was recrystallized from petrol ether/diethyl ether. The product **II** was obtained as a white solid (1.13 g, 4.07 mmol, 89%). ^{1}H NMR (300 MHz, $CDCl_3$): δ [ppm] = 1.49−1.67 (m, 3H, $CH_2^{4'}$, $CH_2^{5'}$, $CH_2^{6'}$), 1.85−2.05 (m, 2H, $CH_2^{4'}$, $CH_2^{5'}$), 2.29−2.43 (m, 1H, $CH_2^{6'}$), 2.98−3.10 (m, 4H, CH_2CH_2Cl), 3.53−3.71 (m, 5H, CH_2Cl, $CH_2^{3'}$), 3.94−4.00 (m, 1H, $CH_2^{3'}$), 5.14−5.18 (m, 1H, $CH^{1'}$), 6.00 (s, 1H, CH^{pz}). ^{13}C NMR (300 MHz, $CDCl_3$): 22.8 (5′-C), 24.9 (4′-C), 29.1 (6′-C), 29.6 (5-$C^{pz}CH_2$), 32.0 (3-$C^{pz}CH_2$), 42.3 (CH_2Cl), 43.5 (CH_2Cl), 67.9 (3′-C), 84.7 (1′-C), 105.4 (4-C^{pz}), 140.4 (5-C^{pz}), 148.8 (3-C^{pz}). MS (ESI+): m/z = 278.2 $[M + H]^+$, 300.2 $[M + Na]^+$. Anal. Calcd (%) for $C_{12}H_{18}Cl_2N_2O$: C, 52.00; H, 6.55; N, 10.11. Found: C, 51.80; H, 6.53; N, 10.00.

3,5-Bis((4-fluorophenylthio)ethyl)-1*H*-pyrazole. A solution of 4-fluorothiophenol (923 mg, 7.2 mmol, 2.0 equiv) in dry THF (30 mL) was deprotonated at −20 °C with a stoichiometric amount of *n*-BuLi (2.5 M in hexane) and stirred for 1 h. A solution of 3,5-bis(chloroethyl)-1-(tetrahydropyran-2-yl)-pyrazole **II** (1.00 g, 3.6 mmol, 1.0 equiv) in dry THF (20 mL) was added, and the resulting solution was stirred at room temperature for 2 days. All volatile materials were then removed in vacuo, and the residue was taken up in CH_2Cl_2 (50 mL) and filtered. The solvent was removed under reduced pressure, and the resulting oil was dissolved in EtOH (40 mL) and ethanolic HCl (20 mL). After stirring for 2 h at room temperature, NaOH (4 M) was added until pH > 9, and the resulting solution was extracted with CH_2Cl_2 (3 × 100 mL). Organic phases were collected and dried over Na_2SO_4, and solvent was evaporated. The crude material was purified via column chromatography using AcOEt/hexane 2:1 as eluent (R_f = 0.58) to give a yellow oil (yield 1.68 g, 69%). ^{1}H NMR (300 MHz, $CDCl_3$): δ [ppm] = 2.88 (t, $^3J_{H-H}$ = 7.5 Hz, 4H, CH_2), 3.11 (t, $^3J_{H-H}$ = 7.5 Hz, 4H, CH_2S), 5.93 (s, 1H, CH^{pz}), 6.98 (t, $^3J_{H-H}$ = $^3J_{H-F}$ = 8.8 Hz, 4H, 3-H^{Ar}), 7.34 (dd, $^3J_{H-H}$ = 8.8 Hz, $^4J_{H-F}$ = 5.4 Hz, 4H, 2-H^{Ar}), 9.75 (b, 1H, NH). ^{13}C NMR (75 MHz, $CDCl_3$): 27.13 (CH_2), 34.71 (CH_2S), 103.35 (4-C^{pz}), 116.25 (d, $^2J_{C-F}$ = 21.75 Hz, 3-C^{Ar}), 130.57 (d, $^4J_{C-F}$ = 3.75 Hz, 1-C^{Ar}), 132.90 (d, $^3J_{C-F}$ = 8 Hz, 2-C^{Ar}), 147.05 (3,5-C^{pz}), 162.08 (d, $^1J_{C-F}$ = 245 Hz, 4-C^{Ar}). ^{19}F NMR (282 MHz, $CDCl_3$): −114.98. ^{1}H NMR (300 MHz, acetone-d_6): δ [ppm] = 2.88 (t, $^3J_{H-H}$ = 7.5 Hz, 4H, CH_2), 3.19 (t, $^3J_{H-H}$ = 7.5 Hz, 4H, CH_2S), 6.00 (s, 1H, CH^{pz}), 7.11 (t, $^3J_{H-H}$ = $^3J_{H-F}$ = 9 Hz, 4H, 3-H^{Ar}), 7.45 (dd, $^3J_{H-H}$ = 9 Hz, $^4J_{H-F}$ = 5.4 Hz, 4H, 2-H^{Ar}), 11.57 (b, 1H, NH). ^{13}C NMR (75 MHz, acetone-d_6): 27.94 (CH_2), 34.65 (CH_2S), 103.26 (4-C^{pz}), 116.77 (d, $^2J_{C-F}$ = 22.5 Hz, 3-C^{Ar}), 132.54 (d, $^4J_{C-F}$ = 3 Hz, 1-C^{Ar}), 132.96 (d, $^3J_{C-F}$ = 7.5 Hz, 2-C^{Ar}), 146.77 (3,5-C^{pz}), 162.53 (d, $^1J_{C-F}$ = 242 Hz, 4-C^{Ar}). ^{19}F NMR (282 MHz, acetone-d_6): −117.65. MS (EI): m/z (%) = 376 [M] (100), 343 (60), 249 [M − SC_6H_4F] (30), 236 [MH − $CH_2SC_6H_4F$] (90). Anal. Calcd (%) for $C_{19}H_{18}F_2N_2S_2$: C, 60.61; H, 4.82; N, 7.44; S, 17.03. Found: C, 60.27; H, 4.75; N, 7.57; S, 17.22.

[AgL]$_3$. Ag_2O (150 mg, 0.65 mmol, 0.6 equiv) was added to a solution of 3,5-bis((4-fluorophenylthio)ethyl)-1*H*-pyrazole (400 mg, 1.06 mmol, 1 equiv) in CH_2Cl_2 (20 mL). The resulting suspension was stirred at 40 °C under exclusion of light for 1 day, then cooled to room temperature, treated with activated carbon, and filtered over Celite. The solvent of the filtrate was removed under reduced pressure to give a beige solid (yield 430 mg, 0.30 mmol, 85%). ^{1}H NMR (500 MHz, $CDCl_3$): δ [ppm] = 2.86 (t, $^3J_{H-H}$ = 7.5 Hz, 4H, CH_2), 3.11 (t, $^3J_{H-H}$ = 7.5 Hz, 4H, CH_2S), 6.03 (s, 1H, CH^{pz}), 6.92 (t, $^3J_{H-H}$ = $^3J_{H-F}$ = 8.5 Hz, 4H, 3-H^{Ar}), 7.26 (dd, $^3J_{H-H}$ = 8.5 Hz, $^4J_{H-F}$ = 5.5 Hz, 4H, 2-H^{Ar}). ^{13}C NMR (125 MHz, $CDCl_3$): 29.25 (CH_2), 35.68 (CH_2S), 101.38 (4-C^{pz}), 116.20 (d, $^2J_{C-F}$ = 21.25 Hz, 3-C^{Ar}), 131.23 (d, $^4J_{C-F}$ = 3.75 Hz, 1-C^{Ar}), 132.26 (d, $^3J_{C-F}$ = 7.5 Hz, 2-C^{Ar}), 152.27 (3,5-C^{pz}), 161.85 (d, $^1J_{C-F}$ = 245 Hz, 4-C^{Ar}). ^{19}F NMR (282 MHz, $CDCl_3$): −115.31. ^{1}H NMR (300 MHz, acetone-d_6): δ [ppm] = 2.83 (t, $^3J_{H-H}$ = 7.25 Hz, 4H, CH_2), 3.17 (t, $^3J_{H-H}$ = 7.2 Hz, 4H, CH_2S), 6.12 (s, 1H, CH^{pz}), 7.02 (t, $^3J_{H-H}$ = $^3J_{H-F}$ = 8.7 Hz, 4H, 3-H^{Ar}), 7.35 (dd, $^3J_{H-H}$ = 8.7 Hz, $^4J_{H-F}$ = 5.1 Hz, 4H, 2-H^{Ar}). ^{19}F NMR (282 MHz, acetone-d_6): −117.45. MS (FD): m/z (%) = 1450.1 $[L_3Ag_3]$ (100). Anal. Calcd (%) for $C_{57}H_{51}F_6N_6S_6Ag_3 \cdot 0.5CH_2Cl_2$: C, 46.27; H, 3.51; N, 5.63; S, 12.89. Found: C, 46.11; H, 3.64; N, 5.58; S, 12.63.

[AuL]$_3$. $AuCl(SMe_2)$ (61 mg, 0.207 mmol, 3.0 equiv) was added to a solution of $[AgL]_3$ (100 mg, 0.069 mmol, 1.0 equiv) in CH_2Cl_2 (20 mL). The mixture was stirred overnight at room temperature under exclusion of light, then treated with activated carbon, and filtered over Celite. The solvent of the filtrate was removed under reduced pressure to give a white solid (yield 106 mg, 0.062 mmol, 89%). ^{1}H NMR (300 MHz, $CDCl_3$): δ [ppm] = 2.89 (t, $^3J_{H-H}$ = 7.2 Hz, 4H, CH_2), 3.21 (t, $^3J_{H-H}$ = 7.2 Hz, 4H, CH_2S), 6.21 (s, 1H, CH^{pz}), 6.97 (t, $^3J_{H-H}$ = $^3J_{H-F}$ = 8.7 Hz, 4H, 3-H^{Ar}), 7.36 (dd, $^3J_{H-H}$ = 8.7 Hz, $^4J_{H-F}$ = 5.1 Hz, 4H, 2-H^{Ar}). ^{13}C NMR (75 MHz, $CDCl_3$): 28.41 (CH_2), 35.45 (CH_2S), 103.68 (4-C^{pz}), 116.33 (d, $^2J_{C-F}$ = 21.75 Hz, 3-C^{Ar}), 130.52 (1-C^{Ar}), 132.80 (d, $^3J_{C-F}$ = 8.25 Hz, 2-C^{Ar}), 150.64 (3,5-C^{pz}), 162.13 (d, $^1J_{C-F}$ = 246 Hz, 4-C^{Ar}). ^{19}F NMR (282 MHz, $CDCl_3$): −114.72. MS (FD): m/z (%) = 1716 $[L_3Au_3]$ (100). Anal. Calcd (%) for $C_{57}H_{51}F_6N_6S_6Au_3$: C, 39.86; H, 2.99; N, 4.89; S, 11.20. Found: C, 40.30; H, 3.42; N, 4.69; S, 10.78.

[CuL]$_3$/[CuL]$_4$. $[Cu(CH_3CN)_4](BF_4)$ (84 mg, 0.267 mmol, 1.0 equiv) was added to a solution of 3,5-bis((4-fluorophenylthio)ethyl)-1*H*-pyrazole (100 mg, 0.266 mmol, 1.0 equiv) in MeOH (10 mL). After 2 min Et_3N (27 mg, 0.267 mmol, 1.0 equiv) was added dropwise to the solution, causing the immediate formation of a precipitate. The suspension was stirred at room temperature for 30 min and then filtered, and the pale green solid was dried in vacuum (yield 430 mg, 0.30 mmol, 85%). ^{1}H NMR (300 MHz, $CDCl_3$): δ [ppm] = 2.72 (b, CH_2 $[CuL]_4$), 2.88 (b, CH_2S $[CuL]_4$), 2.94 (t, $^3J_{H-H}$ = 6.9 Hz, CH_2 $[CuL]_3$), 3.16 (t, $^3J_{H-H}$ = 6.9 Hz, CH_2S $[CuL]_3$), 5.80 (s, 1H, CH^{pz} $[CuL]_4$), 6.00 (s, 1H, CH^{pz} $[CuL]_3$), 6.82 (t, $^3J_{H-H}$ = $^3J_{H-F}$ = 8.4 Hz, 3-H^{Ar} $[CuL]_4$), 6.94 (t, $^3J_{H-H}$ = $^3J_{H-F}$ = 8.4 Hz, 3-H^{Ar} $[CuL]_3$), 7.22−7.32 (m, 2-H^{Ar} $[CuL]_3$ and $[CuL]_4$). ^{19}F NMR (282 MHz, $CDCl_3$): −115.3, −115.2. MS (FD): m/z (%) = 878.1 $[Cu_2L_2]$ (44), 941.1 $[Cu_3L_2]^+$ (37), 1316.1 $[Cu_3L_3]$ (100), 1379.1 $[Cu_4L_3]^+$ (54), 1664.1 (19), 1756.1 $[Cu_4L_4]$ (65), 1819.1 $[Cu_5L_4]^+$ (4).

[Ag$_2$L]$_3$(OTf)$_3$. A solution of AgOTf (32 mg, 124.5 × 10^{-3} mmol, 3.0 equiv) in CH_2Cl_2 (2 mL) and a drop of acetone were added to a solution of $[AgL]_3$ (60 mg, 41.4 × 10^{-3} mmol, 1.0 equiv) in CH_2Cl_2 (5 mL). The resulting solution was stirred overnight at room temperature under exclusion of light, then the solvent was removed under reduced pressure, and the resulting white solid was dried in vacuo (yield 72 mg, 32.4 × 10^{-3} mmol, 78%). Colorless crystals could be obtained by layering hexane over a solution of the complex in CH_2Cl_2. ^{1}H NMR (500 MHz, $CDCl_3$): δ [ppm] = 3.01 (b, CH_2), 3.63 (b, CH_2S), 6.52 (weak, CH^{pz}), 7.02 (b, 3-H^{Ar}), 7.62 (b, 2-H^{Ar}). ^{19}F NMR (471 MHz, $CDCl_3$): −109.83 (Ar−F), −77.77 (SO_3CF_3). ^{1}H NMR (300 MHz, acetone-d_6): δ [ppm] = 3.02 (b, 4H, CH_2), 3.70 (b, 4H, CH_2S), 6.67 (s, 1H, CH^{pz}), 7.17 (t, $^3J_{H-H}$ = $^3J_{H-F}$ = 8.7 Hz, 4H, 3-H^{Ar}), 7.77 (dd, $^3J_{H-H}$ = 8.7 Hz, $^4J_{H-F}$ = 5.1 Hz, 4H, 2-H^{Ar}). ^{13}C NMR (75 MHz, acetone-d_6): 27.41 (CH_2), 40.21 (CH_2S), 117.65 (d, $^2J_{C-F}$ = 21.75 Hz, 3-C^{Ar}), 125.99 (1-C^{Ar}), 136.60 (d, $^3J_{C-F}$ = 8.25 Hz, 2-C^{Ar}), 151.84 (3,5-C^{pz}), 164.19 (d, $^1J_{C-F}$ = 247 Hz, 4-C^{Ar}). ^{19}F NMR (282 MHz, acetone-d_6): −112.78 (Ar−F), −78.32 (SO_3CF_3). MS (FD): m/z (%) = 1815.0 $[Ag_5L_3](OTf)^+$ (95), 2070.9 $[Ag_6L_3](OTf)_2^+$ (100), 2328.8 $[Ag_7L_3](OTf)_3^+$ (29). Anal. Calcd (%) for $C_{60}H_{51}F_{15}N_6O_9S_9Ag_6$: C, 32.45; H, 2.31; N, 3.78; S, 12.99. Found: C, 32.76; H, 2.44; N, 3.81; S, 13.20.

[Ag$_2$L]$_3$(BF$_4$)$_3$. A solution of $AgBF_4$ (24 mg, 0.123 mmol, 3.0 equiv) in CH_2Cl_2 (2 mL) with a drop of acetone was added to a solution of $[AgL]_3$ (60 mg, 0.041 mmol, 1.0 equiv), in CH_2Cl_2 (5 mL). The resulting solution was stirred overnight at room temperature under exclusion of light, becoming a suspension. Solid was filtered and dried in vacuo (yield 63 mg, 0.031 mmol, 75%). Colorless crystals could be obtained from slow evaporation of an acetone solution of the complex. ^{1}H NMR (300 MHz, acetone-d_6): δ [ppm] = 3.05 (b, 4H, CH_2), 3.71 (b, 4H, CH_2S), 6.76 (s, 1H, CH^{pz}), 7.22 (t, $^3J_{H-H}$ = $^3J_{H-F}$ = 8.7 Hz, 4H, 3-H^{Ar}), 7.77 (b, 4H, 2-H^{Ar}). ^{13}C NMR (75 MHz, $CDCl_3$): 27.43 (CH_2), 39.67 (CH_2S), 117.80 (d, $^2J_{C-F}$ = 21.75 Hz, 3-C^{Ar}), 125.33 (1-

dx.doi.org/10.1021/ic5001792 | *Inorg. Chem.* 2014, 53, 2333−2341

C^{Ar}), 136.60 (2-C^{Ar}), 152.24 (3,5-C^{pz}), 164.18 (d, $^1J_{C-F}$ = 247 Hz, 4-C^{Ar}). ^{19}F NMR (282 MHz, acetone-d_6): −150.45 ($^{11}BF_4$), −150.40 ($^{10}BF_4$), −112.80 (Ar−F). MS (FD): m/z (%) = 1752.8 $[Ag_5L_3](BF_4)^+$ (100), 1946.7 $[Ag_6L_3](BF_4)_2^+$ (20), 2040.9 (25), 2234.7 (22). Anal. Calcd (%) for $C_{57}H_{51}B_3F_{18}N_6S_6Ag_6{\cdot}0.5CH_2Cl_2$: C, 33.26; H, 2.52; N, 4.05; S, 9.26. Found: C, 32.93; H, 2.57; N, 3.99; S, 9.23.

$[CuAgL]_3(OTf)_3$. $[AgL]_3$ (80 mg, 0.055 mmol, 1.0 equiv) was added to a suspension of $(CuOTf)_2{\cdot}C_6H_6$ (42 mg, 0.083 mmol, 1.5 equiv) in 10 mL of CH_2Cl_2. The mixture was cooled to −40 °C and stirred under exclusion of light for 3 h and then warmed up to room temperature. The solvent was removed under reduced pressure, and the resulting brownish solid was dried in vacuo (yield 88 mg, 0.042 mmol, 76%). Colorless crystals could be obtained by layering hexane over a solution of the complex in CH_2Cl_2. ^{1}H NMR (500 MHz, $CDCl_3$): δ [ppm] = 3.12 (weak, broad, CH_2), 3.74 (weak, broad, CH_2S), 6.61 (weak, CH^{pz}), 7.01 (broad, 3-H^{Ar}), 7.63 (broad, 2-H^{Ar}). ^{19}F NMR (471 MHz, $CDCl_3$): −110.50 (Ar−F), −109.54 (Ar−F), −77.76 (SO_3CF_3). ^{1}H NMR (500 MHz, acetone-d_6): δ [ppm] = 3.10 (b, 4H, CH_2), 3.75 (b, 4H, CH_2S), 6.68 (s, 1H, CH^{pz}), 7.16 (t, $^3J_{H-H}$ = $^3J_{H-F}$ = 8.5 Hz, 4H, 3-H^{Ar}), 7.80 (b, 4H, 2-H^{Ar}). ^{19}F NMR (471 MHz, $CDCl_3$): −112.12 (Ar−F), −78.46 (SO_3CF_3). MS (FD): m/z (%) = 1680.8 $[Cu_3Ag_2L_3](OTf)^+$ (100), 1938.7 $[Cu_3Ag_3L_3](OTf)_2^+$ (67), 2194.6 $[Cu_3Ag_4L_3](OTf)_3^+$ (15), 1636.9 (23), 1894.8 (22). Anal. Calcd (%) for $C_{60}H_{51}F_{15}N_6S_6Cu_3Ag_3{\cdot}CH_2Cl_2$: C, 33.72; H, 2.46; N, 3.87; S, 13.29. Found: C, 33.35; H, 2.43; N, 4.14; S, 13.29.

$[Cu_2L]_3(OTf)_3$/$[Cu_2L]_4(OTf)_4$. $(CuOTf)_2{\cdot}C_6H_6$ (29 mg, 0.058 mmol, 1.5 equiv) was added to a solution of $[CuL]_3$/$[CuL]_4$ (50 mg, 0.038 mmol, 1.0 equiv) in CH_2Cl_2 (5 mL). The reaction mixture was stirred at room temperature overnight, and then the solvent was removed under reduced pressure and the pale green solid dried in vacuo (yield 51 mg, 0.026 mmol, 69%). ^{19}F NMR (282 MHz, $CDCl_3$): −110.86 (Ar−F), −109.90 (Ar−F), −78.11 (SO_3CF_3). MS (FD): m/z (%) = 1756.1 $[Cu_4L_4]$ (18), 1804.8 $[Cu_6L_3](OTf)_2^+$ (85), 1819.0 $[Cu_5L_4]^+$ (100), 1945.0 (13), 2030.9 (22), 1636.9 (22). Anal. Calcd (%) for $C_{60}H_{51}F_{15}N_6O_9S_6Cu_6{\cdot}2CH_2Cl_2$: C, 35.05; H, 2.61; N, 3.96; S, 13.58. Found: C, 34.61; H, 2.71; N, 4.10; S, 13.97.

$[AuAgL]_3(OTf)_3$. A solution of AgOTf (32 mg, 0.125 mmol, 3.0 equiv) in CH_2Cl_2 (2 mL) and a drop of acetone were added to a solution of $[AuL]_3$ (70 mg, 0.041 mmol, 1.0 equiv) in CH_2Cl_2 (5 mL). The resulting solution was stirred overnight at room temperature under exclusion of light, and then the solvent was removed under reduced pressure and the resulting solid dried in vacuo (yield 78 mg, 0.031 mmol, 77%). ^{19}F NMR (282 MHz, $CDCl_3$): −114.06 (Ar−F), −78.09 (SO_3CF_3). ^{1}H NMR (300 MHz, acetone-d_6): δ [ppm] = 3.24 (b, 4H, CH_2), 3.79 (b, 4H, CH_2S), 6.90 (s, 1H, CH^{pz}), 7.13 (t, $^3J_{H-H}$ = $^3J_{H-F}$ = 8.7 Hz, 4H, 3-H^{Ar}), 7.71 (dd, $^3J_{H-H}$ = 8.7 Hz, $^4J_{H-F}$ = 5.1 Hz, 4H, 2-H^{Ar}). ^{19}F NMR (282 MHz, acetone-d_6): −112.99 (Ar−F), −78.40 (SO_3CF_3). MS (FD): m/z (%) = 1825.1 $[Au_3AgL_3]^+$ (20), 2080.9 $[Au_3Ag_2L_3](OTf)^+$ (100), 2338.8 $[Au_3Ag_3L_3](OTf)_2^+$ (62). Anal. Calcd (%) for $C_{60}H_{51}F_{15}N_6O_9S_6Au_3Ag_3{\cdot}(1/3)C_6H_{14}$ (hexane was used to grow crystals of this complex that were not suitable for X-ray diffraction): C, 30.79; H, 2.54; N, 3.26; S, 11.21. Found: C, 30.72; H, 2.52; N, 3.29; S, 10.91.

$[AuAgL]_3(BF_4)_3$. A solution of $AgBF_4$ (20 mg, 0.103 mmol, 3.0 equiv) in CH_2Cl_2 (2 mL) with a drop of acetone was added to a solution of $[AuL]_3$ (60 mg, 0.035 mmol, 1.0 equiv) in CH_2Cl_2 (5 mL). The resulting solution was stirred overnight at room temperature under exclusion of light, yielding a suspension. The solid was separated by filtration and dried in vacuo (yield 52 mg, 0.023 mmol, 65%). ^{1}H NMR (300 MHz, acetone-d_6): δ [ppm] = 3.18 (t, $^3J_{H-H}$ = 6.0 Hz, 4H, CH_2), 3.71 (t, $^3J_{H-H}$ = 6.0 Hz, 4H, CH_2S), 6.96 (s, 1H, CH^{pz}), 7.19 (t, $^3J_{H-H}$ = $^3J_{H-F}$ = 8.7 Hz, 4H, 3-H^{Ar}), 7.70 (dd, $^3J_{H-H}$ = 8.7 Hz, $^4J_{H-F}$ = 5.1 Hz, 4H, 2-H^{Ar}). ^{13}C NMR (75 MHz, acetone-d_6): 27.53 (CH_2), 39.28 (CH_2S), 103.06 (4-C^{pz}), 117.68 (d, $^2J_{C-F}$ = 13.5 Hz, 3-C^{Ar}), 126.47 (1-C^{Ar}), 135.87 (d, $^3J_{C-F}$ = 5.25 Hz, 2-C^{Ar}), 151.145 (3,5-C^{pz}), 164.09 (d, $^1J_{C-F}$ = 148 Hz, 4-C^{Ar}). ^{19}F NMR (282 MHz, acetone-d_6): −150.81 ($^{11}BF_4$), −150.76 ($^{10}BF_4$), −112.85 (Ar−F). MS (FD): m/z (%) = 1735.0 (20), 1825.1 $[Au_3AgL_3]^+$ (53), 1930.9 (23), 1951.0 (34), 2019.0 $[Au_3Ag_2L_3](BF_4)^+$ (100), 2147.0 (40), 2215.0 $[Au_3Ag_3L_3](BF_4)_2^+$ (20). Anal. Calcd (%) for $C_{57}H_{51}F_{18}B_3N_6S_6Au_3Ag_3$: C, 29.75; H, 2.23; N, 3.65; S, 8.36. Found: C, 29.31; H, 2.34; N, 3.70; S, 8.18.

■ ASSOCIATED CONTENT

Ⓢ Supporting Information

Synthetic procedures and complete experimental details; selected NMR spectra; field-desorption mass spectra; luminescence spectra of $[ML]_3$ and $[MM'L]_3Y_3$; crystallographic details (CIF) and ORTEP plots. This material is available free of charge via the Internet at http://pubs.acs.org.

■ AUTHOR INFORMATION

Corresponding Author

*Tel: +49 551 3933012. Fax: +49 551 3933063. E-mail: franc.meyer@chemie.uni-goettingen.de.

Notes

The authors declare no competing financial interest.

■ ACKNOWLEDGMENTS

Financial support by the Georg-August-University, the DFG (International Research Training Group IGRK 1422 "Metal Sites in Biomolecules: Structures, Regulation and Mechanisms"; see www.biometals.eu; support of the PhD work of S.M. and N.K.) and and the Fonds der Chemischen Industrie (PhD scholarship for N.K.) is gratefully acknowledged.

■ REFERENCES

(1) La Monica, G.; Ardizzoia, G. A. *Prog. Inorg. Chem.* **1997**, *46*, 151.
(2) Mohamed, A. A. *Coord. Chem. Rev.* **2010**, *254*, 1918.
(3) Halcrow, M. A. *Dalton Trans.* **2009**, 2059.
(4) (a) Dias, H. V. R.; Gamage, C. S. P. *Angew. Chem., Int. Ed.* **2007**, *46*, 2192. (b) Tekarli, S. M.; Cundari, T. R.; Omary, M. A. *J. Am. Chem. Soc.* **2008**, *130*, 1669. (c) Omary, M. A.; Elbjeirami, O.; Gamage, C. S. P.; Sherman, K. M.; Dias, H. V. R. *Inorg. Chem.* **2009**, *48*, 1784. (d) Rawashdeh-Omary, M. A.; Rashdan, M. D.; Dharanipathi, S.; Elbjeirami, O.; Ramesh, P.; Dias, H. V. R. *Chem. Commun.* **2011**, *47*, 1160.
(5) Dias, H. V. R.; Diyabalanage, H. V. K.; Eldabaja, M. G.; Elbjeirami, O.; Rawashdeh-Omary, M. A.; Omary, M. A. *J. Am. Chem. Soc.* **2005**, *127*, 7489.
(6) Ardizzoia, G. A.; Cenini, S.; La Monica, G.; Masciocchi, N.; Moret, M. *Inorg. Chem.* **1994**, *33*, 1458.
(7) Maspero, A.; Brenna, S.; Galli, S.; Penoni, A. *J. Organomet. Chem.* **2003**, *672*, 123.
(8) (a) Raptis, R. G.; Fackler, J. P. *Inorg. Chem.* **1988**, *27*, 4179. (b) Yang, G.; Raptis, R. G. *Inorg. Chim. Acta* **2003**, *352*, 98. (c) Fujisawa, K.; Ishikawa, Y.; Miyashita, Y.; Okamoto, K. *Inorg. Chim. Acta* **2010**, *363*, 2977.
(9) (a) Vorontsov, I.; Kovalevsky, A.; Chen, Y.-S.; Graber, T.; Gembicky, M.; Novozhilova, I.; Omary, M.; Coppens, P. *Phys. Rev. Lett.* **2005**, *94*, 193003. (b) Grimes, T.; Omary, M. A.; Dias, H. V. R.; Cundari, T. R. *J. Phys. Chem. A* **2006**, *110*, 5823.
(10) Yang, G.; Raptis, R. G. *Inorg. Chem.* **2003**, *42*, 261.
(11) (a) Dias, H. V. R.; Diyabalanage, H. V. K.; Eldabaja, M. G.; Elbjeirami, O.; Rawashdeh-Omary, M. A.; Omary, M. A. *J. Am. Chem. Soc.* **2005**, *127*, 7489. (b) Omary, M. A.; Rawashdeh-Omary, M. A.; Gonser, M. W. A.; Elbjeirami, O.; Grimes, T.; Cundari, T. R.; Diyabalanage, H. V. K.; Gamage, C. S. P.; Dias, H. V. R. *Inorg. Chem.* **2005**, *44*, 8200. (c) Zhang, J.-X.; He, J.; Yin, Y.-G.; Hu, M.-H.; Li, D.; Huang, X.-C. *Inorg. Chem.* **2008**, *47*, 3471.
(12) (a) Jozak, T.; Sun, Y.; Schmitt, Y.; Lebedkin, S.; Kappes, M.; Gerhards, M.; Thiel, W. R. *Chem.—Eur. J.* **2011**, *17*, 3384. (b) Gao, G.-F.; Li, M.; Zhan, S.-Z.; Lv, Z.; Chen, G.-H.; Li, D. *Chem.—Eur. J.* **2011**, *17*, 4113. (c) Duan, P.-C.; Wang, Z.-Y.; Chen, J.-H.; Yang, G.; Raptis, R. G. *Dalton Trans.* **2013**, *42*, 14951.

(13) (a) Scheele, U. J.; Georgiou, M.; John, M.; Dechert, S.; Meyer, F. *Organometallics* **2008**, *27*, 5146. (b) Stollenz, M.; John, M.; Gehring, H.; Dechert, S.; Grosse, C.; Meyer, F. *Inorg. Chem.* **2009**, *48*, 10049. (c) Georgiou, M.; Wöckel, S.; Konstanzer, V.; Dechert, S.; John, M.; Meyer, F. *Z. Naturforsch.* **2009**, *64b*, 1542. (d) Klingele, J.; Dechert, S.; Meyer, F. *Coord. Chem. Rev.* **2009**, *253*, 2698.
(14) Meyer, F.; Jacobi, A.; Zsolnai, L. *Chem. Ber./Recl.* **1997**, *130*, 1441.
(15) Jahnke, A. C.; Pröpper, K.; Bronner, C.; Teichgräber, J.; Dechert, S.; John, M.; Wenger, O. S.; Meyer, F. *J. Am. Chem. Soc.* **2012**, *134*, 2938.
(16) Gondoh, A.; Koike, T.; Akita, M. *Inorg. Chim. Acta* **2011**, *374*, 489.
(17) Röder, J. C.; Meyer, F.; Pritzkow, H. *Organometallics* **2001**, *20*, 811.
(18) Krishantha, D. M. M.; Gamage, C. S. P.; Schelly, Z. A.; Dias, H. V. R. *Inorg. Chem.* **2008**, *47*, 7065.
(19) Falvello, L. R.; Forniés, J.; Martín, A.; Navarro, R.; Sicilia, V.; Villarroya, P. *Chem. Commun.* **1998**, 2429.
(20) Forniés, J.; Martín, A.; Sicilia, V.; Martín, L. F. *Chem.—Eur. J.* **2003**, *9*, 3427.
(21) Brandi-Blanco, P.; Sanz Miguel, P. J.; Lippert, B. *Eur. J. Inorg. Chem.* **2012**, *2012*, 1122.
(22) Bondi, A. *J. Phys. Chem.* **1964**, *68*, 441.
(23) A Cu···Cu separation of 2.905 Å was reported in the following: Singh, K.; Long, J. R.; Stavropoulos, P. *J. Am. Chem. Soc.* **1997**, *119*, 2942. A Ag···Ag separation of 2.971 Å was reported in the following: Mohamed, A. A.; Pérez, L. M.; Fackler, J. P. *Inorg. Chim. Acta* **2005**, *358*, 1657.
(24) A very short unsupported Cu···Cu separation of 2.672 Å was reported for a dinuclear guanidine chloride complex: Chiarella, G. M.; Melgarejo, D. Y.; Rozanski, A.; Hempte, P.; Perez, L. M.; Reber, C.; Fackler, J. P. *Chem. Commun.* **2010**, *146*, 136.
(25) For complexes $[Ag_2L]_3(OTf)_3$ and $[AuAgL]_3(OTf)_3$ the C_6H_4F-4 could not be detected in ^{19}F DOSY experiments, likely because of the broadness of the peaks in ^{19}F NMR; however the very small diffusion coefficent of the triflate groups clearly indicates that they are bound to the complex.
(26) In the non-normalized spectra the maximum intensity of the emission at 430 nm is around 10 times lower than the maximum intensity of the peak at 620 nm (see Figure S35 in the Supporting Information).
(27) Crystalline material of $[CuAgL]_3(OTf)_3$ was used for the luminescence measurements. Furthermore, comparison of the FD mass spectra of $[Cu_2L]_3(OTf)_3$, $[Ag_2L]_3(OTf)_3$, and $[CuAgL]_3(OTf)_3$ showed that the latter did not contain any admixture of the homometallic compounds. Thus we exclude the possibility that the two emission peaks are due to a mixture of homo- and heterometallic complexes.

dx.doi.org/10.1021/ic5001792 | *Inorg. Chem.* 2014, 53, 2333−2341